Technical Digest Topical Meeting "Nonlinear Guided Waves and their Applications (NLGW '04)", Toronto/Canada, March 2004, paper TuC 43

Lateral displacement of beams in transversely engineered Ti:PPLN waveguides

Fabio Baronio, Costantino De Angelis
Istituto Nazionale per la Fisica della Materia, Università di Brescia, via Branze 38, 25123 Brescia, Italy
Tel:+39 030 3715437,Fax:+39 030 380014,deangeli@ing.unibs.it

Paul-Henri Pioger, Vincent Couderc, Alain Barthélémy
I.R.C.O.M., Faculté des Sciences, 123 av. A. Thomas, 87060 Limoges, France
Tel :+33 555457256,Fax :+33 555457514,abarth@ircom.unilim.fr.

Yoohong Min, Victor Quiring, Wolfgang Sohler
Angewandte Physik, Universitat Paderborn, 33095 Paderborn, Germany
Tel:+49-5251-60-2714,Fax:+49-5252-60-3422,sol_ws@physik.uni-paderborn.de

Abstract: The spatial dynamics of beams at the interface between two PPLN regions with different poling period is considered. We demonstrate numerically and experimentally intensity and phase-mismatch dependent spatial control of picosecond pulses at 1549nm.

OCIS codes: 190.4420, 070.4340, 060.5530

1 Introduction

Following the milestone research of Bloembergen and Pershan [1] and of Kaplan [2], the propagation of light in the vicinity of an interface between two nonlinear dielectrics has been widely studied in the past four decades (see [3-4] and references therein). However few experimental results have been provided over the past decades. In the framework of quadratic nonlinear media, quasi-phase matching (QPM) technique can be exploited to realize engineered nonlinear structures. This opens a whole range of new possibilities, which have become experimentally feasible with the progress of a reproducible fabrication of periodically poled lithium niobate (PPLN). Spatial nonlinear reflection, tunneling, resonant trapping and emission have been predicted in transversely engineered QPM gratings [5,6]. Recently, spatial nonlinear deflection [7] and soliton reflection [8,9] at nonlinear interfaces have been observed.

Here, we report on a new engineered PPLN sample with two laterally interfaced PPLN regions with different poling periods. We show the spatial dynamics of beams that propagate along the phase-mismatched nonlinear interface. We experimentally observed intensity and phase-mismatch (temperature or wavelength) dependent spatial displacement of picosecond pulses at 1549nm. Numerical simulations that correspond to the experiments are also presented.

2 Experimental set-up and Numerical Modeling

The experiments were performed in a 80mm long Ti:$LiNbO_3$ planar waveguide fabricated in a z-cut substrate by indiffusion of 70nm thick, vacuum-deposited Ti-layer at 1064°C. Two transversely interfaced micro-domain structures of Λ=16.74 μm (P1) and of Λ=16.67 μm (P2) periodicity have been generated after waveguide fabrication by electric field assisted poling. Thus, the sample exhibited a transition (the nonlinear phase-mismatched interface) between periodically poled regions (see Fig. 1). The sample was inserted in a temperature stabilized oven to allow operation at elevated temperatures (phase matching occurred at T=216°C in P1 and at T=198°C in P2); in this way, photorefractive effects ("optical damage") could be minimized. Moreover, temperature-tuning of the phase-matching conditions became possible. An all-fiber laser system was used as the source of 5 ps pulses (FWHM in intensity) at 1549 nm (FF) of 1.7 nm spectral bandwidth and of a peak power of a few kilowatts at 20 MHz repetition rate. The thickness of the waveguide permitted the propagation of a single TM_0 mode of 4μm width at the FF; several TM modes are supported at the second harmonic (SH), but only the TM_0 of 3μm width is efficiently pumped by the TM_0 at the FF. The laser beam was shaped in a highly elliptical spot, nearly gaussian in profile, with a spot of 4μm (FWHM in intensity) along the guided dimension and with a spot of 80μm along the perpendicular direction, and was polarized parallel to the z axis of the PPLN for access to the material's largest quadratic nonlinear coefficient $\chi^{(2)}_{zzz}=(2d_{33})$. The spatial beam profiles were recorded by scanning a magnified image of the pattern with

a photodiode.

As to numerics, the electric fields E_1 and E_2, at ω_0 (FF) and $2\omega_0$ (SH) respectively, with $\omega_0=2\pi c/\lambda_0$ and λ_0=1549nm free space wavelength, propagating in the y direction, can be written as $E_1(x,y,z,t)=1/2[m_1(z)a_1(x,y,t)\exp(-j(\beta_{\omega 0}y+\omega 0t))+cc]$ and $E_2(x,y,z,t)=1/2[m_2(z)a_2(x,y,t)\exp(-j(\beta_{2\omega 0}y+2\omega 0t))+cc]$ with $m_1(z)$ and $m_2(z)$ the mode profiles, $a_1(x,y,t)$ and $a_2(x,y,t)$ the slowly varying envelopes. Averaging over the QPM periods, at the lowest order $a_1(x,y,t)$ and $a_2(x,y,t)$ obey the nonlinear coupled equations:

$$
\begin{aligned}
& j\frac{\partial a_1}{\partial y} - jb'_{w_0}\frac{\partial a_1}{\partial t} - \frac{b''_{w_0}}{2}\frac{\partial^2 a_1}{\partial t^2} + \frac{1}{2b_{w_0}}\frac{\partial^2 a_1}{\partial x^2} + \frac{c^{(2)}w_0}{2cn_{w_0}}\frac{\int m_2|m_1|^2 dz}{\int |m_1|^2 dz}a_2 a_1^* e^{-j\Delta ky} = 0 \\
& j\frac{\partial a_2}{\partial y} - jb'_{2w_0}\frac{\partial a_2}{\partial t} - \frac{b''_{2w_0}}{2}\frac{\partial^2 a_2}{\partial t^2} + \frac{1}{2b_{2w_0}}\frac{\partial^2 a_2}{\partial x^2} + \frac{c^{(2)}w_0}{2cn_{2w_0}}\frac{\int m_2|m_1|^2 dz}{\int |m_2|^2 dz}a_1^2 e^{j\Delta ky} = 0
\end{aligned}
\qquad (1)
$$

where β represents the propagation constant, β' the inverse group velocity, β'' the inverse group-velocity dispersion; n is the refractive index, $\chi^{(2)} = (2/\pi)\chi^{(2)}_{zzz}$ is the nonlinear coefficient. $\Delta k = 2\beta_{\omega_0} - \beta_{2\omega_0} + K_S$ is the mismatch, where $K_S = 2\pi/\Lambda$. We assumed that the nonlinear interface is located at x = 0. We employ a finite-difference vectorial mode solver to determine the linear propagation properties in the slab waveguide, i.e., the mode profiles, β_{ω_0}, $\beta_{2\omega_0}$, β'_{ω_0}, $\beta'_{2\omega_0}$, β''_{ω_0} and $\beta''_{2\omega_0}$. The crystal length corresponded to 3.7 times the FF diffraction length and to 5.6 times the group velocity mismatch length between FF and SH; the dispersive terms can be neglected. Finally, using a finite-difference beam propagation technique, we solved the nonlinear coupled equations (Eqs. (1)).

3 Results

Experiments and numerical simulations were carried out launching the FF input beam along the nonlinear interface, varying input pulse power and phase-mismatch conditions via temperature of the sample, keeping fixed the temporal and spatial widths of the injected FF pulse.

At first, we launched the FF beam, at a given input displacement, close to and along the interface, at the temperature of 204°C (that represents $\Delta kL_{P1}=20\pi$ and $\Delta kL_{P2}=-10\pi$) varying the input intensity. In the quasi linear regime, at low intensity, the beam broadened because of diffraction inside the crystal. By increasing the incident intensity, in nonlinear regime, we succeeded in exciting spatial self-trapped beams and we observed their spatial shift. In Fig. 2, typical numerical and experimental results are shown. The beams experienced an intensity dependent effective spatial acceleration and consequently spatial velocity in the transverse dimension (x) towards the P1 region. The higher the input intensity the higher the lateral velocity.

Then, we launched the FF beam, at a given input displacement, close to and along the interface, at the input intensity of 150MW/cm^2 varying the temperature of the sample. In Fig. 3, typical numerical and experimental results are shown. At the temperature of 204°C (that represents $\Delta kL_{P1}=20\pi$ and $\Delta kL_{P2}=-10\pi$) the self-trapped beam is significantly deflected towards the P1 region. On the contrary, at the temperature of 185°C (that represents $\Delta kL_{P1}=50\pi$ and $\Delta kL_{P2}=30\pi$) the self-trapped beam is deflected towards the P2 region.

This phenomenon can be attributed to the existence of an intensity and phase-mismatch dependent potential barrier induced by the effective nonlinear interface. The intensity of the potential barrier is inversely proportional to the separation distance between the input beam and the interface.

4 Conclusions

We numerically and experimentally showed that a phase-mismatch boundary between periodically poled regions leads to the spatial deflection of beams. The intensity and phase-mismatch (temperature or wavelength) control of the deflection phenomenon opens new scenarios for ultrafast all-optical devices.

References

1. N. Bloembergen and P.S. Pershan, Phys. Rev. **128,** 606 (1962).
2. A.E. Kaplan, Sov. Phys. JETP **45**, 896 (1977).
3. V. Shadrivov and A. A. Zharov, J. Opt. Soc. Am. B **19**, 596 (2002).
4. A.B. Aceves, J. V. Moloney, and A.C. Newell, Phys. Rev. A **39**, 1809 (1989).
5. C. Balslev Clausen and L. Torner, Phys. Rev. Lett. **81,** 790 (1998).
6. F. Baronio and C. De Angelis, IEEE J. Quantum Electron. **38**, 1309 (2002).
7. F. Baronio, C. De Angelis, P. Pioger, V. Couderc,, A. Barthelemy, Y. Min, V. Quiring, and W. Sohler, Opt. Lett. **28**, 2348 (2003).
8. P. Pioger, V. Couderc, L. Grossard, A. Barthelemy, F. Baronio and C. De Angelis, *in technical digest of European Quantum Electronics Conference* (Munich, June 2003), paper EP1-5-THU.
9. L.Jankovic, H. Kim, G. Stegeman, S. Carrasco, L. Torner, M. Kats, Opt. Lett. **28**, 2103 (2003).

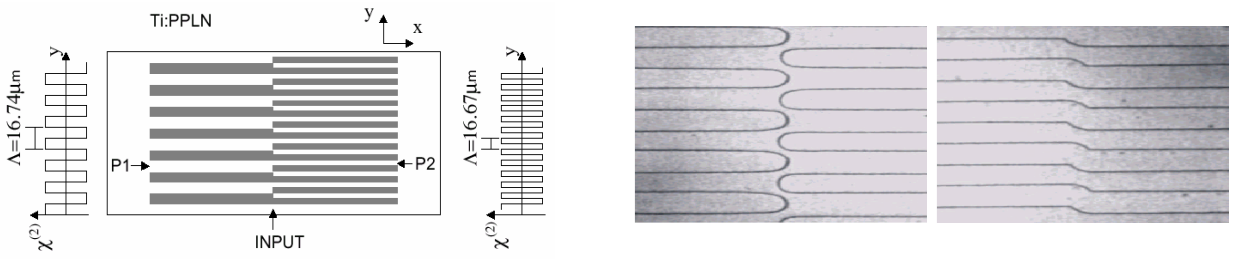

Fig. 1. Left, schematic of the nonlinear geometry: transversely interfaced micro-domain structures of Λ=16.74 μm (P1) and of Λ=16.67 μm (P2) periodicity. Right, photographs of portions of the PPLN chip, showing the phase-mismatched nonlinear interface.

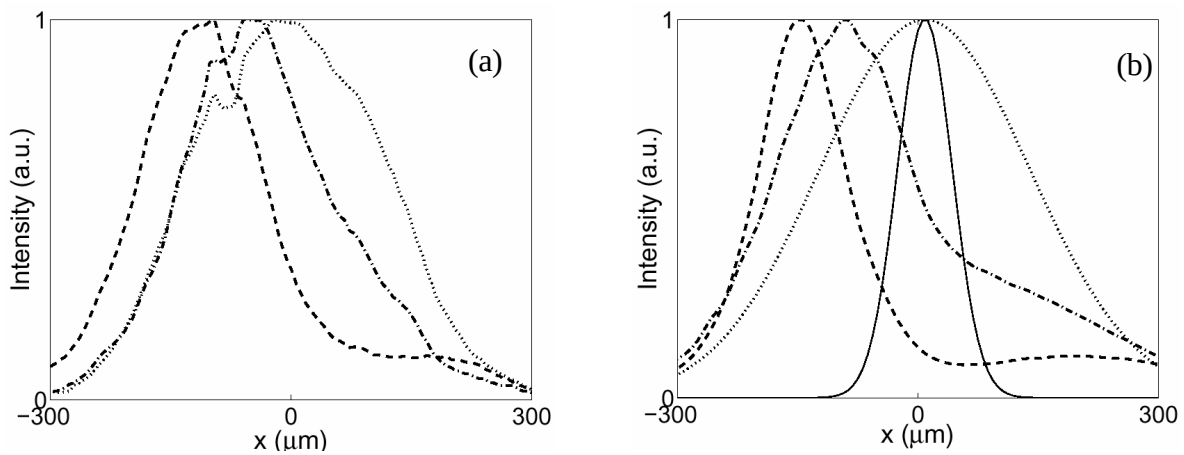

Fig. 2. (a), measured and (b), calculated spatial profiles of the FF output beam taken at T=204°C for three input intensities: I=0.1MW/cm^2, linear regime (dotted curve); I=38MW/cm^2 (dashed-dotted curve); I=167MW/cm^2 (dashed curve); the solid curve in (b) represents input profile.

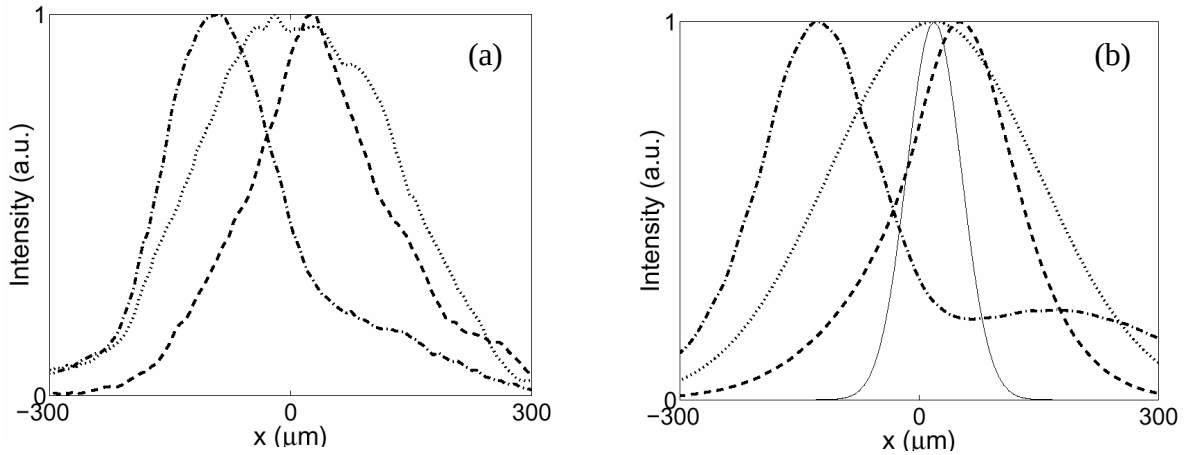

Fig. 3. (a), measured and (b), calculated spatial profiles of the FF output beam taken at I=150MW/cm^2 for two temperatures: T=204°C (dashed-dotted curve); T=185°C (dashed curve); the dotted curve represents the output profile in linear regime, the solid curve in (b) represents the input profile.